19. P. R. Castillo and M. S. Pringle, *Eos* **72**, 300 (1991).
20. Y. Lancelot, paper presented at the Reunion Hot Spot Meeting, Reunion Island (1991).
21. E. L. Winterer *et al.*, *Init. Rep. Deep Sea Drilling Proj.* **17**, 145 (1973).
22. J. A. Tarduno, W. V. Sliter, T. J. Bralower, M. McWiliams, I. Premoli Silva, J. Ogg, *Geol. Soc. Am. Bull.* **101**, 1306 (1989).
23. J. A. Tarduno, *Geology* **18**, 683 (1990). A brief reversed interval in the K-N Superchron (ISEA) is based on the co-occurrence of the *Globigerrinelloides algerianus* foraminiferal Zone and both reversed inclinations and proxy declination values from DSDP Site 463. The occurrence of such brief reversed intervals is an area of ongoing study. Alternatively, the *G. algerianus* Zone can be used for the correlations discussed.
24. J. Thiede *et al.*, *Init. Rep. Deep Sea Drilling Proj.* **62**, 43 (1981); T. L. Vallier and W. S. Jefferson, *ibid.*, p. 545; J. R. Hein and E. Vanek, *ibid.*, p. 559.
25. W. B. Harland, A. V. Cox, P. G. Llewellyn, C. A. G. Pickton, A. G. Smith, R. Walters, *A Geologic Time Scale* (Cambridge Univ. Press, New York, 1982).
26. W. B. Harland, R. L. Armstrong, A. V. Cox, L. E. Craig, A. G. Smith, D. G. Smith, *A Geologic Time Scale 1989* (Cambridge Univ. Press, New York, 1990). The duration assigned to the Aptian in this time scale (12.5 million years) may be an overestimate. Study of sedimentary cycles suggests a duration of some 8 million years [T. D. Herbert, E. Erba, I. Premoli Silva, A. G. Fischer, J. Park, *Abstr. 28th Int. Geol. Congr.* **2**, 51 (1989)]. In the highest sedimentation rate site available (DSDP Site 463), reversed polarity chron M0 postdates the first occurrence of *H. similis* and *R. irregularis*, indicating an age entirely within the early Aptian (*22*). The Harland *et al.* (1989) time scale changes the standard correlation of foraminiferal zone to stage, correlating *H. similis* to the Barremian rather than the Aptian. An equivalent change relative to stage is not applied to the nannofossil zonation.
27. P. R. Castillo, R. W. Carlson, R. Batiza, *Earth Planet. Sci. Lett.* **103**, 200 (1991).
28. R. L. Larson, *Geology* **19**, 547 (1991).
29. G. Schubert and D. Sandwell, *Earth Planet. Sci. Lett.* **92**, 234 (1989).
30. B. Parsons and J. G. Sclater, *J. Geophys. Res.* **82**, 803 (1977).
31. It is possible that the OJP formed at least in part on zero-age crust. Therefore, our volumes are underestimates. In addition, losses due to subduction may result in an underestimate of volume by a factor of 2. The volume of sediments corresponding to thicknesses greater than those at the base depths should also be subtracted; because these corrections are less than 10% of the volumes corrected for preexisting crust, they are not considered here.
32. DSDP Site 288 may record sporadic volcanism from Aptian to Coniacian times; moreover basalt termed "basement" at the bottom of Site 803 could be as young as early Cenomanian. Because the former is not recorded at our proximal or distant reference sites and the latter is not recorded at Ontong Java Sites 289 or 807, we infer that post-Aptian eruptions are volumetrically minor.
33. F. Stacey and D. Loper, *Phys. Earth Planet. Inter.* **53**, 167 (1988).
34. R. T. Merrill and P. L. McFadden, *Science* **248**, 345 (1990); P. L. McFadden and R. T. Merrill, *J. Geophys. Res.* **89**, 3354 (1984). Although the increase in reversal frequency before the K-N Superchron is less accurate because of the increasing uncertainty in absolute ages back in time, a comparison of the two times scales previously discussed reveals that these uncertainties are likely to change the slope of the increase but unlikely to remove it completely.
35. P. L. McFadden and R. T. Merrill, *Phys. Earth Planet. Inter.* **43**, 22 (1986).
36. V. Courtillot and J. Besse, *Science* **237**, 1140 (1987).
37. G. M. Jones, *J. Geophys. Res.* **82**, 1703 (1977).
38. W. J. Morgan, *Geol. Soc. Am. Mem.* **132**, 7 (1972).
39. R. G. Gordon and L. J. Henderson, in preparation.
40. R. A. Duncan and D. A. Clague, in *The Ocean Basin and Margins*, vol. 7, *The Pacific Ocean*, A. Nairn, F. G. Stehli, S. Uyeda, Eds. (Plenum, New York, 1985), pp. 89–121.
41. P. Lonsdale, *J. Geophys. Res.* **93**, 3078 (1988); A. B. Watts, J. K. Weissel, R. A. Duncan, R. L. Larson, *ibid.*, p. 3051.
42. R. G. Gordon, *ibid.* **95**, 8397 (1990).
43. M. Kono, M., *Init. Rep. Deep Sea Drilling Proj.* **55**, 737 (1980).
44. Lithostratigraphy: M. E. Tornaghi, I. Premoli Silva, M. Ripepe, *Riv. Ital. Paleontol. Stratigr.* **95**, 223 (1989); biostratigraphy: E. Erba, *ibid.* **94**, 249 (1988); magnetostratigraphy: W. Lowrie, W. Alvarez, I. Premoli Silva, S. Monechi, *Geophys. J. R. Astron. Soc.* **60**, 263 (1980).
45. R. Coccioni, O. Nesci, M. Tramontana, F. C. Wezel, E. Moretti, *Geol. Soc. Italy Bull.* **106**, 183 (1987).
46. W. V. Sliter, *Geology* **17**, 909 (1989).
47. J. A. Tarduno, M. McWilliams, M. G. Debiche, W. V. Sliter, M. C. Blake, Jr., *Nature* **317**, 345 (1985).
48. B. U. Haq, J. Hardenbol, P. R. Vail, *Science* **235**, 1156 (1987).
49. H. C. Jenkyns, *J. Geol. Soc. London* **137**, 171 (1980); E. R. Force, *Eos* **65**, 18 (1984); R. E. Sheridan, *Paleoceanography* **2**, 97 (1987).
50. High spreading rates can also lead to sea level rise, but high rates previously postulated during the middle Cretaceous might be in part due to a pulse of faster spreading during the early Aptian. Until short polarity events are located on the sea floor (*23*), such a pulse of spreading cannot be evaluated.
51. S. O. Schlanger, *Init. Rep. Deep Sea Drilling Proj.* **33**, 161 (1976).
52. R. S. Cockerham and J. M. Hall, *J. Geophys. Res.* **81**, 4207 (1976).
53. An interval of reversed polarity within the volcaniclastics postulated by the shipboard party was not confirmed by subsequent sampling and was likely due to either core pieces accidentally inverted during recovery or a previously unrecognized short polarity event in the early Aptian; see J. A. Tarduno, thesis, Stanford University, Stanford, CA (1987).
54. The location of a present-day hot-spot trail linked to Manihiki Plateau has yet to be identified. Although it is possible that Manihiki Plateau was formed by a separate plume source, the extrapolated position of Site 317 falls close to the Pacific-Phoenix-Farallon-plate triple junction [see E. L. Winterer, in *The Geophysics of the Pacific Ocean Basin and its Margin*, G. H. Sutton, M. H. Manghnani, R. Moberly, Eds. (*Geophys. Monogr. 19*, American Geophysical Union, Washington, DC, 1976), pp. 269–278]. Alternatively, Manihiki Plateau may have been constructed from the same broad plume source as the OJP.
55. R. A. Duncan and M. A. Richards, *Rev. Geophys.* **29**, 31 (1991). Kerguelen Plateau may be related to the same mantle plume source responsible for the Rajmahal Traps which have a radiometric data of 117 Ma, consistent with an early Aptian age. See A. Baksi, *Geology* **16**, 758 (1988).
56. M. Storey *et al.*, *Nature* **338**, 574 (1989).
57. M. A. Arthur, R. L. Larson, W. E. Dean, *Eos* **71**, 1660 (1991).
58. R. M. Leckie, *Palaeogeogr. Palaeoclimatol. Palaeoecol.* **73**, 107 (1989).
59. We thank W. Berger, P. Castillo, Y. Gallet, R. Larson, H. Staudigel, D. Sandwell, D. Mueller, and the Leg 130 shipboard scientific party for helpful discussions and reviews. This work was supported by the U.S. Science Support Program and the National Science Foundation.

16 May 1991; accepted 29 July 1991

Oxygen Isotope Zoning in Garnet

C. Page Chamberlain* and Mark E. Conrad

Oxygen isotope zoning was examined within garnet with the use of the stable isotope laser probe. Four metamorphic garnets from the regional metamorphic terrane in Vermont and the skarn deposit at Carr Fork, Utah, were examined and were found to be concentrically zoned in $\delta^{18}O$ values. The largest variations in $\delta^{18}O$ values were observed in the regional metamorphic garnets, where $\delta^{18}O$ values change by 3 per mil from core to rim. These oxygen isotope zoning profiles reflect the changes in the $\delta^{18}O$ values of the rocks during garnet growth, which are caused by infiltration of fluids and by dehydration reactions during metamorphism.

U NTIL RECENTLY, ANALYSIS OF THE oxygen isotopic composition of rocks has been restricted to the study of whole rock powders and mineral separates. However, the advent of the stable isotope laser probe (*1*) and the ion microprobe makes it possible to examine both oxygen isotope zoning within minerals (*2*) and the oxygen isotope composition of minerals in situ within a rock (*1*). These technological breakthroughs are leading to significant advances in the understanding of fluid-rock interactions, the scale of isotopic equilibrium (*2*), and kinetic isotopic effects (*3*). Because $\delta^{18}O$ variations reflect the na-

ture of fluid-rock interactions, $\delta^{18}O$ zoning within minerals provides important information about the temporal nature of fluid migration during mineral growth. Such information is of fundamental importance in understanding the geochemical processes that occur in igneous and metamorphic rocks. We have used the stable isotope laser probe to study oxygen isotope zoning in metamorphic garnets from both regional and contact metamorphic terranes.

Many garnets are zoned in cations (Fe, Mg, Mn, and Ca) (*4*), trace elements (*5*), and radiogenic isotopes (*6, 7*). Zonation profiles of these elements have been used to determine variations in pressure (*P*), temperature (*T*), and time (*t*) during garnet growth (*6–9*). Studies of $\delta^{18}O$ zoning in garnets, coupled with this *P-T-t* information, have the potential to provide a monitor

Department of Earth Sciences, Dartmouth College, Hanover, NH 03755.

*To whom correspondence should be addressed.

of fluid-rock interaction during garnet growth because $\delta^{18}O$ is a sensitive indicator of fluid sources.

We examined garnets from two distinct metamorphic settings: a skarn deposit at Carr Fork, Utah, and a Barrovian-style regional metamorphic terrane in eastern Vermont. These metamorphic settings were selected because garnets from the skarn deposit clearly grew at a time when the rocks were open to infiltrating fluids, whereas the garnets from the regional metamorphic terrane may have been closed to infiltrating fluids. Oxygen isotope profiles should reflect these open-system or closed-system behaviors. In addition, the regional metamorphic garnets were chosen because they are already well characterized (6, 10, 11). The regional metamorphic garnets are from the Gassetts schist at the northern end of the Chester dome and the Pinney Hollow Formation (12) from the western side of the Athens dome. These garnets grew during the Acadian orogeny as the rocks were deformed into a series of west vergent nappes or thrusts and later structural domes (6, 13).

Oxygen was extracted from the garnets with the use of a stable isotope laser probe located at Dartmouth College. This apparatus is similar to that described by Sharp (1), but differs in its laser beam delivery system. A CO_2 laser beam was allowed to burn completely through 0.5-mm sections of garnet in a BrF_5 atmosphere. In order to avoid sputtering of the samples, the laser was operated at 10 W in a continuous mode. After freezing the sample on a liquid nitrogen trap, the oxygen was passed through a mercury transfer pump to re-
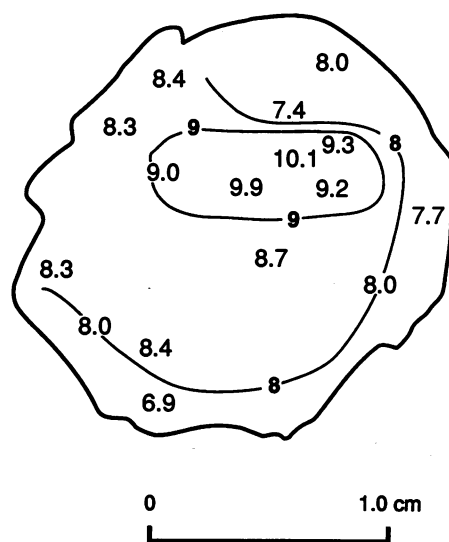
move any fluorine gas. The oxygen was then converted to CO_2 on a hot carbon rod. The typical sample consisted of 1 to 2 μmol of CO_2. The CO_2 samples were analyzed on a Finnigan Delta E stable isotope mass spectrometer.

To evaluate the accuracy and precision of the oxygen isotope analyses of garnet, we analyzed a homogeneous garnet standard using (i) the conventional BrF_5 method (14); (ii) the laser to sample completely small (~1 mg) chips of garnet; and (iii) the laser to sample the garnet in situ. The mean $\delta^{18}O$ (15) values of the standard garnets were 6.53 ± 0.24 (1 σ) with the conventional method, 6.33 ± 0.26 with the com-

plete laser analyses, and 6.17 ± 0.28 with in situ laser analyses.

The garnet crystals, which range from 1.0 to 3.0 cm in diameter, were analyzed in 0.5- to 1.0-mm spots in the crystals. The individual analyses were taken at 2- to 3-mm intervals across each garnet. It was necessary to keep the spots separated by at least this distance because the laser beam affects the isotopic composition of garnet in a narrow radius around the laser spot. Care was also taken to avoid mineral inclusions. In addition, all of the garnets were examined for major element zoning with an electron microprobe. Both the Pinney Hollow and Gassetts garnets (10) are Fe^{2+}-rich and concentrically zoned such that Mn and Ca decrease whereas Fe and Mg increase from core to the rim. The garnets from Carr Fork are andradites (Fe^{3+}- and Ca-rich) and contain only minor amounts of Mn, Mg, and Fe^{2+} (16).

All of the garnets examined are concentrically zoned in oxygen isotopes. The regional metamorphic garnets from Vermont are the most strongly zoned (as much as 3 per mil), whereas the skarn garnets have only relatively minor zoning (~0.5 per mil) (Figs. 1 to 4). In addition, the $\delta^{18}O$ zoning in the garnets are significantly different in all three rocks studied. The Carr Fork garnet has a homogeneous core and a slight decrease in $\delta^{18}O$ in the outer 3 mm of the garnet. The $\delta^{18}O$ values of garnet from the Gassetts schist are ~2 per mil lower in the rim than the core. Two separate garnets from the Pinney Hollow Formation that are 1 cm apart in the same section of rock have similar zoning profiles and show a 3 per mil increase in $\delta^{18}O$ values from core to rim. The $\delta^{18}O$ values at the cores of both garnets increase from 6 per mil in the cores to a high of ~9 per mil at the rims.

Fig. 2. Oxygen isotope zoning profile of a garnet from the Gassetts Schist. Numbers represent $\delta^{18}O$ analyses and light lines are contours of the $\delta^{18}O$ values of the garnet.
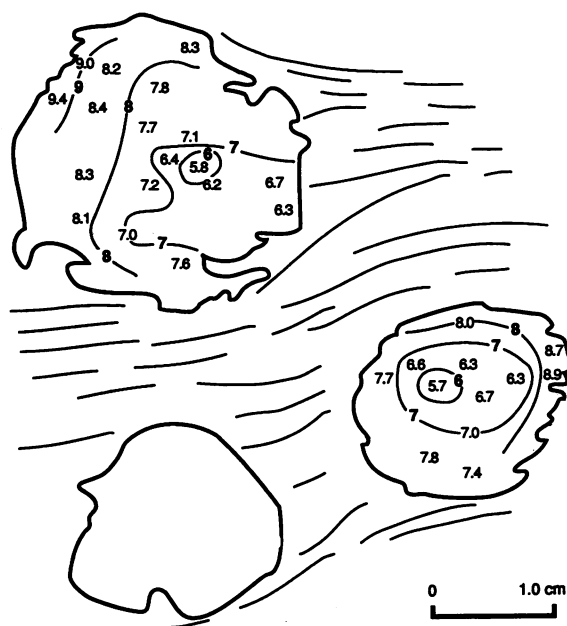
Fig. 1. Oxygen isotope zoning profiles in two garnets from the Pinney Hollow Formation. The heavy lines show the outlines of three garnets in the section and the lighter wavy lines in the matrix show the mica and chlorite foliation. Numbers within garnets are the results of in situ analyses of the $\delta^{18}O$ values of the garnet. Light lines within garnets are contours of $\delta^{18}O$ values.
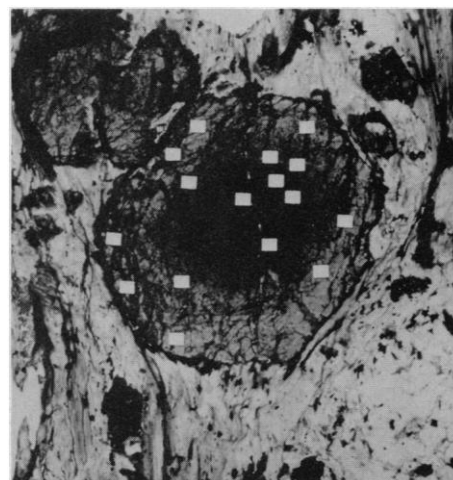
Fig. 3. Photograph of the garnets from the Gassetts schist. Dots show the location of analyses. Section is 2.75 cm across.
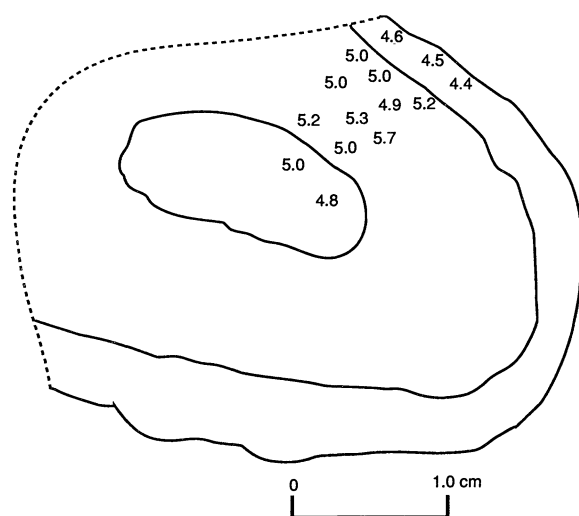
Fig. 4. Oxygen isotope zoning in a garnet from the Carr Fork skarn deposit. Numbers represent results of the in situ analyses of the $\delta^{18}O$ values of the garnet. Solid lines represent optical zoning observed in garnet and the dashed line is a broken edge of the garnet.

$\delta^{18}O$ whole rock and mineral separate data. Second, our results indicate that the oxygen isotope zoning profiles in garnet can be used to determine the temporal nature of fluid flow. In the past, fluid flow in metamorphic rocks has been quantitatively described in terms of time-integrated fluid fluxes or fluid-rock ratios (28, 29). Although these measurements are useful, they provide little information about the interval of time over which fluids migrated within the rocks. This information is imperative in determining the effects of fluids on the thermal and mechanical history of metamorphic terranes. Oxygen isotope zoning studies of garnet, coupled with quantitative P-T-t data, will provide this necessary and important information.

We believe that the oxygen isotope profiles are the result of fluid-rock interaction and net transfer reactions during garnet growth. It is unlikely that the zoning profiles were significantly influenced by diffusion of oxygen isotopes within the garnet nor were they an artifact resulting from the analysis of oxygen from minerals included within garnet. The effects of diffusion can be dismissed because the diffusivity of oxygen in garnet is extremely low at metamorphic temperatures (17, 18). Significant contamination due to mineral inclusions is also unlikely, as each garnet was examined petrographically, and relatively inclusion-free spots were chosen for analysis. Although there were large amounts of fine inclusions in both the Pinney Hollow and Gassetts garnets, and some inclusions were undoubtedly included in the analyses, they could not have produced the variations observed (19).

In the Pinney Hollow garnets, the oxygen isotope zoning can be explained by continuous loss of volatiles during Acadian metamorphism (Fig. 1). The garnets grew over an approximate 10-million-year interval (6), presumably by a prograde devolatilization reaction that involved the breakdown of chlorite (20). This reaction released relatively large amounts of H_2O having a lower $\delta^{18}O$ value than that of the rock (21, 22). Continuous release of this relatively light isotopic fluid during the devolatilization resulted in an increase in the $\delta^{18}O$ values of the garnet by as much as 2 per mil during garnet growth (21, 22). The isotopic zoning within the garnet, therefore, resulted from the garnet rim maintaining equilibrium with the evolving fluids during garnet growth. The similar oxygen isotope profiles of the two garnets in this section suggests that they were in oxygen isotope equilibrium during growth.

The zoning profiles in the garnet from the Gassetts schist, however, cannot be the re-sult of devolatization reactions (Figs. 2 and 3). As with the Pinney Hollow garnets, release of H_2O at the temperatures at which this garnet formed should have produced a fluid with a lower $^{18}O/^{16}O$ ratio relative to that of the rocks; this process would have caused the $\delta^{18}O$ values of garnets to increase during growth. However, the Gassetts garnet shows a 2 per mil decrease in $\delta^{18}O$ values from core to rim. This profile could reflect infiltration of a relatively low $\delta^{18}O$ fluid during the later stages of garnet growth, which has previously been suggested by other petrologic (23) and stable isotopic studies (24) of these rocks.

The Carr Fork garnets were formed in a metasomatic hydrothermal system in the contact aureole of the Bingham stock, Utah. Petrologic and isotopic studies show that the fluids that infiltrated these rocks during their formation were dominantly magmatic in origin. However, the very latest stages of the hydrothermal system involved infiltration of meteoric waters as the rocks cooled (16, 25). The oxygen isotopic composition of the Carr Fork garnet is consistent with this model (Fig. 4). The lack of $\delta^{18}O$ zoning in its core suggests that most of the garnet grew under a relatively restricted interval of temperature and fluid composition, presumably as magmatic fluids infiltrated the rocks. The slight decrease in $\delta^{18}O$ values in the outer few millimeters of the garnet could be either the result of the influx of the later meteoric fluids or the result of a temperature decrease.

The strong zoning of these garnets in oxygen isotopes has two important implications for stable isotopic studies. First, the magnitude of the zoning in $\delta^{18}O$ values within a single garnet crystal is as large as observed variations in $\delta^{18}O$ values of whole rocks from isotopic studies of regional metamorphic terranes (26, 27), and this should be taken into consideration when interpreting

REFERENCES AND NOTES

1. Z. D. Sharp, *Geochim. Cosmochim. Acta* **38**, 21 (1990).
2. J. W. Valley and C. M. Graham, *Geol. Soc. Am. Abstr. Prog.* **22**, A348 (1990).
3. Z. D. Sharp, *Geology* **19**, 653 (1991).
4. R. J. Tracy et al., *Am. Mineral.* **61**, 762 (1976).
5. D. D. Hickmott et al., *Geology* **15**, 573 (1987).
6. J. N. Christensen, J. L. Rosenfeld, D. J. DePaolo, *Science* **244**, 1465 (1989).
7. D. Vance and R. K. O'Nions, *Earth Planet. Sci. Lett.* **97**, 227 (1990).
8. F. S. Spear and J. Selverstone, *Contrib. Mineral. Petrol.* **83**, 348 (1983).
9. J. Selverstone et al., *J. Petrol.* **25**, 501 (1984).
10. A. B. Thompson et al., *Am. J. Sci.* **277**, 1152 (1977).
11. A. B. Thompson et al., *ibid.*, p. 1124.
12. The garnets from the Pinney Hollow Formation examined in this study are the same as those studied by Christensen et al. (6). These garnets were originally thought to belong to the Ottauquechee Formation, but remapping by J. Rosenfeld shows that they are from the Pinney Hollow Formation.
13. J. L. Rosenfeld, *Geol. Soc. Am. Spec. Pap.* **129** (1970).
14. R. N. Clayton and T. K. Mayeda, *Geochim. Cosmochim. Acta* **27**, 43 (1963).
15. All oxygen isotope values are reported as $\delta^{18}O$ relative to SMOW (standard mean ocean water). $\delta^{18}O_{sample} = [(O^{18}/O^{16}_{sample} - O^{18}/O^{16}_{SMOW})/(O^{18}/O^{16}_{SMOW})] \times 10^3$.
16. W. W. Atkinson and M. T. Einaudi, *Econ. Geol.* **73**, 1326 (1978).
17. R. A. N. Coghlan, thesis, Brown University, Providence, RI (1990).
18. The characteristic diffusive length-scale for oxygen in garnet for 400 million years at 500°C and a diffusivity of 2.63×10^{-25} cm^2/s (17) is 0.6 μm.
19. The possibility that the observed variations in $\delta^{18}O$ values within the garnets are due to removal of oxygen from mineral inclusions can be tested by calculating the effects of analyzing inclusions in the garnets from the Pinney Hollow Formation. The dominant minerals included in these garnets are quartz and ilmenite. To produce a 3 per mil increase in $\delta^{18}O$ values in the rim of the garnet would require that 60% of the oxygen be derived from quartz. Likewise, to produce a 3 per mil decrease in $\delta^{18}O$ values in the garnet core 60% of the oxygen would have to be from ilmenite inclusions.
20. The presumed reaction that formed garnet in the Pinney Hollow Formation is: 2 chlorite + 4 quartz = 3 garnet + Tk + 8 water. Tk is the exchange component FeSiAl$_{-2}$ found in chlorite and mica.
21. C. P. Chamberlain et al., *Contrib. Mineral. Petrol.* **105**, 322 (1990).
22. Using the method of Chamberlain et al. (21), we find that the $\delta^{18}O$ value of garnet increases on the order of 2 per mil from core to rim due to net transfer reaction effects. The $\delta^{18}O$ value of the fluid is ~5 per mil less than that of the quartz, the dominant mineral in the rock.
23. J. M. Ferry, *J. Petrol.*, in press.

24. L. Stern et al., in preparation.
25. M. T. Einaudi et al., Econ. Geol. 73, 1215 (1978).
26. S. M. Wickham and H. P. Taylor, Contrib. Mineral. Petrol. 91, 122 (1985).
27. C. P. Chamberlain and D. Rumble III, J. Petrol 29, 1215 (1989).
28. H. P. Taylor, Jr., J. Geol. Soc. London 133, 509 (1977).
29. M. J. Bickle and J. Baker, Earth Planet. Sci. Lett. 97, 78 (1990).

Visual Observations of the Amorphous-Amorphous Transition in H2O Under Pressure

OSAMU MISHIMA, K. TAKEMURA, K. AOKI

The vapor-deposited low-density amorphous phase of H_2O was directly compressed at 77 kelvin with a diamond-anvil cell, and the boundary between the low-density amorphous phase and the high-density amorphous phase was observed while the sample was warmed under compression. The transition from the low-density amorphous phase to the high-density amorphous phase was distinct and reversible in an apparently narrow pressure range at ~130 to ~150 kelvin, which provided experimental evidence for polymorphism in amorphous H_2O.

ONE MIGHT THINK THAT, AS WITH liquids, amorphous solids contract gradually when compressed slowly. However, recent high-pressure experiments revealed polymorphism in an amorphous material and sharp transitions between the amorphs (1–5). Compressed in a piston-cylinder apparatus at 77 K, low-density amorphous (lda) H_2O (~0.94 g/cm^3 at 1 bar) transforms into a high-density amorphous (hda) phase (~1.17 g/cm^3 at 1 bar) at ~6 kbar (3). A sharp volume decrease of ~22% at ~6 kbar showed that the transformation is apparently a first-order transition (3, 6). However, the possibility that the transformation is a structural relaxation process was suggested by Moynihan (7), implying that the amorphous H_2O might be the sole phase. The polymorphism in amorphous H_2O was therefore questioned. Because H_2O is an important material, we endeavored to reconfirm the polymorphism in amorphous H_2O. To do this, we compressed vapor-deposited lda H_2O directly with a diamond-anvil cell (DAC) and observed the lda-hda boundary to examine the polymorphism in the amorphous H_2O.

The lda H_2O used in our experiment was prepared as follows. Water vapor, introduced through a metal tube after passing through a small hole (120 μm in diameter), was slowly deposited (<~200 μm/hour) in a vacuum onto a copper-block substrate (80 to 105 K) that was set down in a borosilicate-

glass bottle immersed in liquid nitrogen. The temperature of the nozzle (278 to 288 K) and that of the substrate were monitored during the deposition, and a transparent H_2O film (<~100 μm thick) was obtained.

Formation of the lda H_2O was confirmed from the heat evolved in the lda→Ic transition (8, 9). The H_2O film (~100 μm thick) was deposited, in the same way as above, onto a thin copper plate (~2 cm^2 by 0.1 mm) attached to the substrate. The film on the copper plate was warmed from ~77 to 273 K. During the warming (~5°C per second), we detected one quick increase in temperature of several degrees at ~170 K, which we attributed to the crystallization of a substantial amount of the lda H_2O to form ice Ic. The increase in temperature at ~170 K was reproducible in all of several measured runs. Comparison with smooth warming curves obtained for ice Ih proved the formation of the lda H_2O.

To detect the lda-hda boundary, we compressed the lda H_2O directly between diamond anvils without a gasket (10). The lda powder with a mean grain size of ~10 μm, made by scraping the thin lda film off the substrate, was loaded in the DAC [Merrill-Bassett type with three pinching screws (11) and 1-mm-diameter anvil faces]. The handling was done while the sample was wet

with liquid nitrogen. The temperature of the lda H_2O was carefully kept below ~110 K. When we squeezed the lda powder in the DAC by turning the screws at 77 K, voids at grain boundaries vanished in the central region of the sample. Then the DAC was clamped with the screws under compression and warmed at a rate of ~1.5°C per minute (Fig. 1, a through e). Above ~130 K (12), there appeared a boundary (labeled D in Fig. 1) in the peripheral region in the sample. We examined the boundary by tilting the incident direction of transmitting or reflecting light applied to the sample. Judging from a change of contrast of the boundary, we found that the peripheral boundary D corresponded to a rather sharp change in density. Several other boundaries appeared above ~150 K, indicating the appearance of high-pressure ice phases (Fig. 1, d and e).
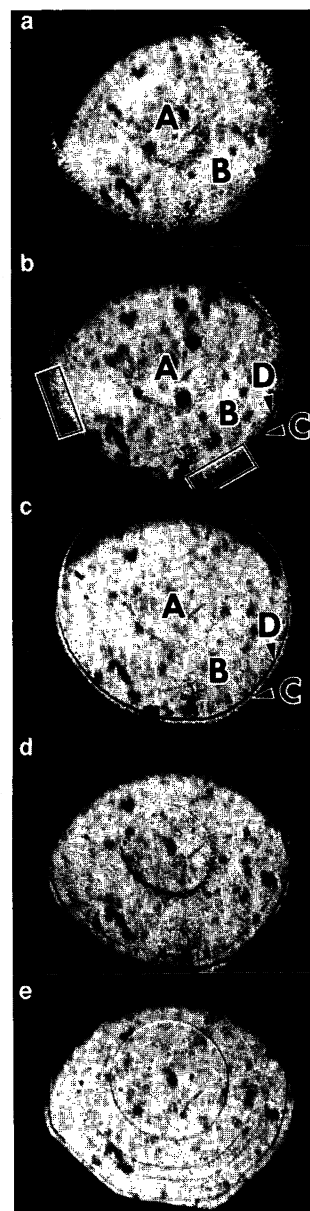
O. Mishima and K. Takemura, National Institute for Research in Inorganic Materials, 1-1, Namiki, Tsukuba, Ibaraki 305, Japan.
K. Aoki, National Chemical Laboratory for Industry, 1-1, Higashi, Tsukuba, Ibaraki 305, Japan.

Fig. 1. Microscopic photographs of the compressed lda H_2O during the warming: (**a**) ~105 K; (**b**) ~130 K; (**c**) ~145 K; (**d**) ~160 K; and (**e**) ~200 K. A is the crystalline phase (probably ice VII'); B is the hda phase; C is the lda phase; D is the peripheral boundary corresponding to the lda-hda boundary. The four boundaries of (e) (~200 K) correspond, presumably, to ice Ih→II→V→VI→VIII from the edge to the center.